

Supporting Information for:

# A Five-Coordinate Heme Dioxygen Adduct Isolated within a Metal-Organic Framework

John S. Anderson,<sup>†</sup> Audrey T. Gallagher,<sup>†</sup> Jarad A. Mason,<sup>‡</sup> and T. David Harris<sup>\*,†</sup>

<sup>†</sup>Department of Chemistry, Northwestern University, Evanston, Illinois 60208-3113

<sup>‡</sup>Department of Chemistry, University of California, Berkeley, California 94720-1460, United States

Email: dharris@northwestern.edu

*J. Am. Chem. Soc.*

---

## Table of Contents

<b>Experimental Section</b>	<b>S2</b>
<b>Figure S1:</b> Thermal ellipsoid plots for <b>1</b> and <b>2</b>	<b>S5</b>
<b>Figure S2:</b> Residual electron density plots for <b>1</b> and <b>2</b>	<b>S6</b>
<b>Figure S3:</b> IR spectra of PCN-224 and <b>1</b>	<b>S7</b>
<b>Figure S4:</b> Diffuse reflectance UV-Vis spectra of PCN-224 and <b>1</b>	<b>S8</b>
<b>Figure S5:</b> N <sub>2</sub> adsorption data for <b>1</b>	<b>S9</b>
<b>Figure S6:</b> Determination of BET surface area for <b>1</b>	<b>S10</b>
<b>Figure S7:</b> O <sub>2</sub> adsorption data for <b>1</b>	<b>S11</b>
<b>Figure S8:</b> Mössbauer spectra for <b>2</b>	<b>S12</b>
<b>Table S1:</b> Crystal table for <b>1</b>	<b>S13</b>
<b>Table S2:</b> Crystal table for <b>2</b>	<b>S14</b>
<b>Table S3:</b> Langmuir fit parameters for <b>1</b> + O <sub>2</sub>	<b>S15</b>
<b>References</b>	<b>S15</b>

## Experimental Section

**General Considerations.** Unless otherwise noted, all materials and chemicals were purchased from commercial suppliers and used without further purification. Additionally, unless otherwise noted, all manipulations were carried out under an atmosphere of N<sub>2</sub> using either standard Schlenk techniques or in a Vacuum Atmospheres Nexus II glovebox. All glassware was dried at 150 °C and allowed to cool under vacuum prior to use. All solvents were dried on a solvent purification system from Pure Process Technology and stored under N<sub>2</sub> over 4 Å molecular sieves. Effective removal of O<sub>2</sub> and H<sub>2</sub>O from solvents was verified using a standard solution of Na benzophenone ketyl radical anion. The material PCN224 was prepared as reported with minor modifications to the literature procedure.<sup>1</sup>

**PCN-224.** ZrCl<sub>4</sub> (0.21 g, 0.90 mmol), benzoic acid (7.0 g, 60 mmol), and tetracarboxyphenylporphyrin (0.070 g, 0.088 mmol) were suspended in DMF (14 mL) in a 20 mL pyrex vial with a teflon-lined cap in air. The mixture was then heated at 130 °C for 3 days to give red, cubic crystals. The vial was allowed to cool for 1 hour, and the mother liquor was then decanted. The remaining solid was washed with DMF (6 x 5 mL) and MeOH (3 x 5 mL). The material was then activated for 12 hours at 150 °C under vacuum to yield PCN-224 (0.070 g, 0.017 mmol, 57%). Large single crystals, suitable for X-ray diffraction, were grown via an identical procedure using benzoic acid (3.5 g, 30 mmol) and acetic acid (3.5 mL, 58 mmol). UV-Vis (diffuse reflectance, nm): 440, 522, 556, 597, 651. The PXRD and IR data for this compound are identical to those previously reported.<sup>1</sup>

**PCN-224Fe<sup>II</sup> (1).** A 20 mL vial was charged with PCN-224 (0.106 g, 0.0259 mmol), FeBr<sub>2</sub> (0.267 g, 0.903 mmol), DMF (5 mL), and 2,6-lutidine (1 g). This vial was then sealed and heated for 12 hours at 150 °C. After this time, the supernatant was decanted off and the remaining solid was washed with DMF (6 x 5 mL) by soaking the material for 30 min at 150 °C and decanting. The solid was then washed with THF (3 x 5 mL) by soaking the material for 1 hour and then decanting off the supernatant. The remaining solid was then dried for 12 hours at 150 °C under vacuum to yield **1** as a dark purple crystalline solid (0.109 g, 0.0256 mmol, 99%). ICP-AES for Zr:Fe mass ratio: Expected 4.9; Found 4.7. FT-IR (KBr pellet, cm<sup>-1</sup>): 1600 (s), 1520 (s), 1407 (vs), 1273 (s), 1205 (w), 1177 (w), 1122 (w), 1071 (w), 1000 (s), 869 (m), 828 (w), 800 (w), 775 (m), 720 (m), 687 (w), 651 (w), 487 (m). UV-Vis (diffuse reflectance, nm): 442, 550, 660, 743.

**PCN-224FeO<sub>2</sub> (2).** Compound **2** for analysis was generated by exposing freshly activated PCN-224Fe<sup>II</sup> to ca. 1 atm of O<sub>2</sub>. Gas sorption samples were activated on a Micromeritics ASAP 2020 at 150 °C until an outgas rate of less than 1 mTorr/minute was observed prior to O<sub>2</sub> uptake measurements. Samples for single-crystal X-ray diffraction were prepared by cooling activated crystals of **1** to -78 °C and then introducing 1 atm of O<sub>2</sub> for 1 minute. After this time, the crystals were transported while cold to the diffractometer where they were rapidly coated in

Paratone-N oil and mounted. Samples for Mössbauer analysis were prepared as a sample of activated **1** in a delrin cup. This material was evacuated for 15 minutes on a Schlenk line before 1 atm of O<sub>2</sub> was added. The sample was left under dynamic O<sub>2</sub> for an additional 15 minutes before being coated in Paratone-N oil and sealed. The sample was then cooled to -78 °C for 10 minutes before being removed from the Schlenk line and frozen in liquid nitrogen.

**X-ray Structure Determination.** Single crystals of **1** and **2** suitable for X-ray analysis were coated in Paratone-N oil and mounted on a Micro Mounts™ rod attached to a goniometer head. The crystallographic data were collected at 100 K on a Bruker APEX II diffractometer equipped with CuK $\alpha$  microsource. Raw data were integrated and corrected for Lorentz and polarization effects using Bruker APEX2 v. 2009.1.4 Absorption corrections were applied using SADABS.<sup>2</sup> Space group assignments were determined by examination of systematic absences, E-statistics, and successive refinement of the structures. Structures were solved and refined with SHELXL<sup>3</sup> operated with the Olex2 interface with the aid of standard restraints.<sup>4,5</sup> Disorder was modeled in structures of both **1** and **2**. Additionally, residual electron density found in the difference Fourier map was removed using the solvent mask protocol included in Olex2. This residual electron density likely arises from either residual solvent, or partial occupation of a separate morphology of the previously reported, and closely related, compound MOF-525.<sup>6</sup> The Fe ellipsoids of both **1** and **2** are consistent with complete occupation of the site by Fe. The elongation of the ellipsoids is consistent with disorder in and out of the plane which is reflected throughout the porphyrin scaffold.

For clarity, a more detailed discussion of the structure of **2** is provided here: Upon refinement, a strong Q-peak was located ca. 1.8 Å from the Fe center and was assigned as an O atom. A subsequent refinement resulted in an O atom with reasonable displacement parameters. At this point, only minimal amounts of electron density were found near the Fe-bound-O atom, likely due to the disorder of the second O atom. Upon application of a solvent mask, two distinct Q-peaks appeared ca. 1.2 Å from the Fe-bound O atom. These peaks were assigned as the disordered second O atom and refinement resulted in reasonable atomic displacement parameters for this atom. The structure was finished and refined without any restraints on the distances or angles in the Fe-O<sub>2</sub> unit.

**Gas Adsorption Measurements.** Crystalline material was transferred into a pre-weighed analysis tube which was then sealed with a Transeal. Activation and analysis was then performed on a Micromeritics ASAP 2020 instrument. The samples were activated at 150 °C until an outgas rate of less than 1 mTorr/minute was observed. After activation, the samples were weighed to determine the final mass of analyte. The sample was checked to ensure the outgas rate remained below 1 mTorr/minute. Oxygen uptake was measured using volumetric methods and the free space of all samples was determined with UHP He prior to analysis. Temperature control was provided with a variety of cold baths: liquid nitrogen for 77 K, liquid nitrogen/pentane for 141 K, liquid nitrogen ethanol for 156 K, dry ice/isopropanol for 195 K, dry ice/acetonitrile for 226 K, and an ice bath for 273 K. Measurements at 141 and 156 K were collected only to 1.59 and 14.9 kPa, respectively, corresponding to the maximum amount of time during which a constant

temperature of the bath could be ensured. The experimental BET surface area of 2901(32) m<sup>2</sup> g<sup>-1</sup> is close to the accessible surface area<sup>7</sup> of 3402 m<sup>2</sup> g<sup>-1</sup> that is calculated from the crystal structure of **1**.

**Other Physical Measurements.** UV-Visible spectra were recorded on a Cary 5000 spectrometer equipped with an integrating sphere for diffuse reflectance measurements. Samples were prepared by a 10 fold dilution of the compound in KBr followed by mulling of the mixture with mineral oil. The collected data were treated with background and baseline subtractions. Inductively coupled plasma atomic emission (ICP-AE) spectra were collected with a Varian VISTA ICP-OES instrument. Infrared spectra were recorded on a Bruker Alpha FTIR spectrometer with the samples prepared as KBr pellets. Zero-field <sup>57</sup>Fe Mössbauer spectra were obtained at 100 K with a constant acceleration spectrometer and a <sup>57</sup>Co/rhodium source. Prior to measurements, the spectrometer was calibrated at 295 K with  $\alpha$ -iron foil. Samples were prepared under nitrogen, or in the case of **2** oxygen, atmosphere and frozen in liquid nitrogen prior to handling in air. Each sample contained approximately 100 mg of compound (~4 mg of Fe). All spectra were analyzed using the WMOSS Mössbauer Spectral Analysis Software (www.wmoss.org). A fit to a minor species in the spectrum of **2** gives an isomer shift of  $\delta = 0.25$  (fixed) mm/s with a quadrupole splitting of  $\Delta E_Q = 0.66(9)$  mm/s at 100 K, consistent with 7(2)% of high-spin Fe<sup>III</sup> containing impurity in the sample.

**Calculation of Predicted Difference in Binding Enthalpy.** As an approximation of the difference in binding enthalpy due to the difference in redox potential between a four-coordinate heme center and a five-coordinate imidazole-ligated heme center, the Nernst equation was applied:  $\Delta G = -nF\Delta E$ , where F is Faraday's constant and  $n$  is the number of electrons involved in the process. We are furthermore specifically considering the difference between two separate reactions, allowing us to rewrite the equation as  $\Delta\Delta G = -nF\Delta\Delta E$ . Utilizing the definition that  $\Delta G = \Delta H - \Delta ST$ , we assume that the entropic difference in O<sub>2</sub> binding to these two Fe centers is similar, such that the entropic contribution cancels out and the equation can simplify to  $\Delta\Delta H = -nF\Delta\Delta E$ . Using a value of  $\Delta E = 0.25$  V, determined from reported Fe<sup>II/III</sup> couples for (TPP)Fe<sup>8</sup> and 2-[8-{*N*-(2-methylimidazolyl)}octanoyloxymethyl]-5,10,15,20-tetrakis( $\alpha$ ,  $\alpha$ ,  $\alpha$ ,  $\alpha$ -*o*-pivalamidophenyl)porphinatoiron(II),<sup>9</sup> and assuming a one electron process, a value of  $\Delta\Delta G = -24$  kJ/mol is obtained. Equivalently, one can input the experimentally determined value of  $\Delta\Delta H$  of -34 kJ/mol and predict a  $\Delta\Delta E$  of 0.310 V, again close to the reported  $\Delta\Delta E$  of 0.250 V.

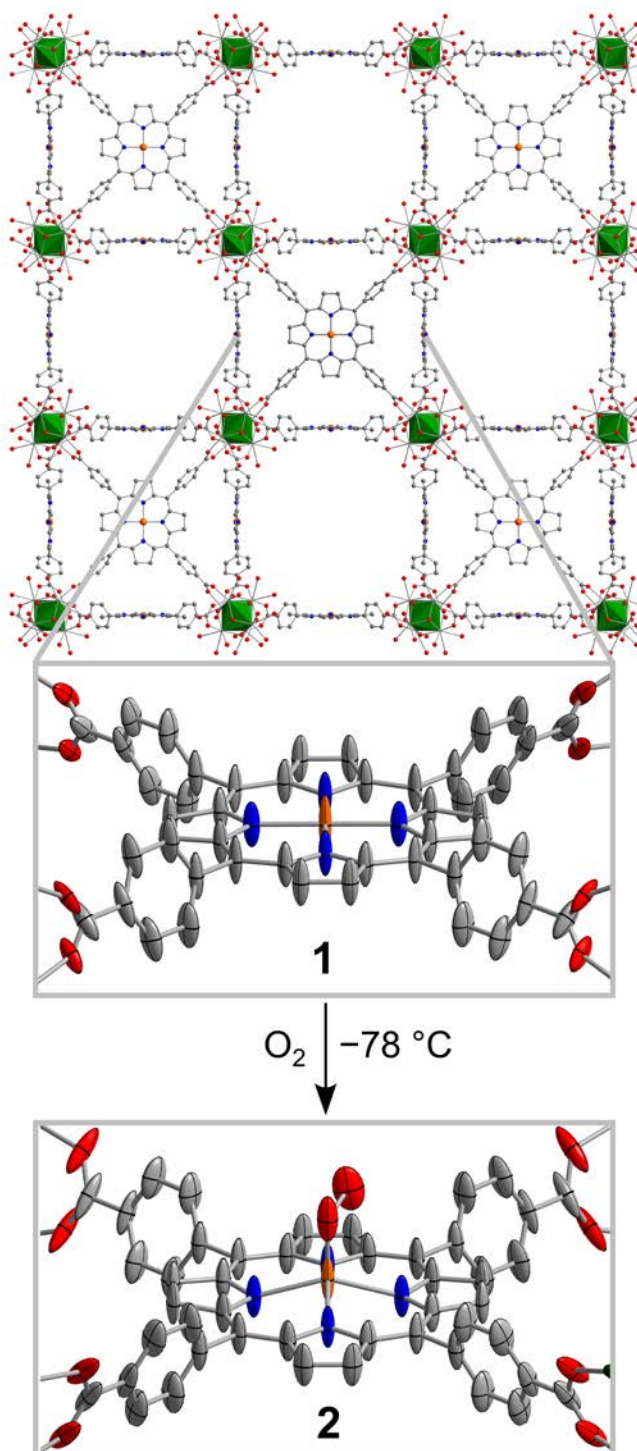


**Figure S1** / Reaction of PCN-224Fe<sup>II</sup> (**1**) with O<sub>2</sub> at -78 °C to form PCN-224FeO<sub>2</sub> (**2**). Ellipsoids are shown at 30%. Green octahedra represent Zr atoms; orange, blue, red, and gray ellipsoids represent Fe, N, O, and C atoms, respectively; hydrogen atoms are omitted for clarity.

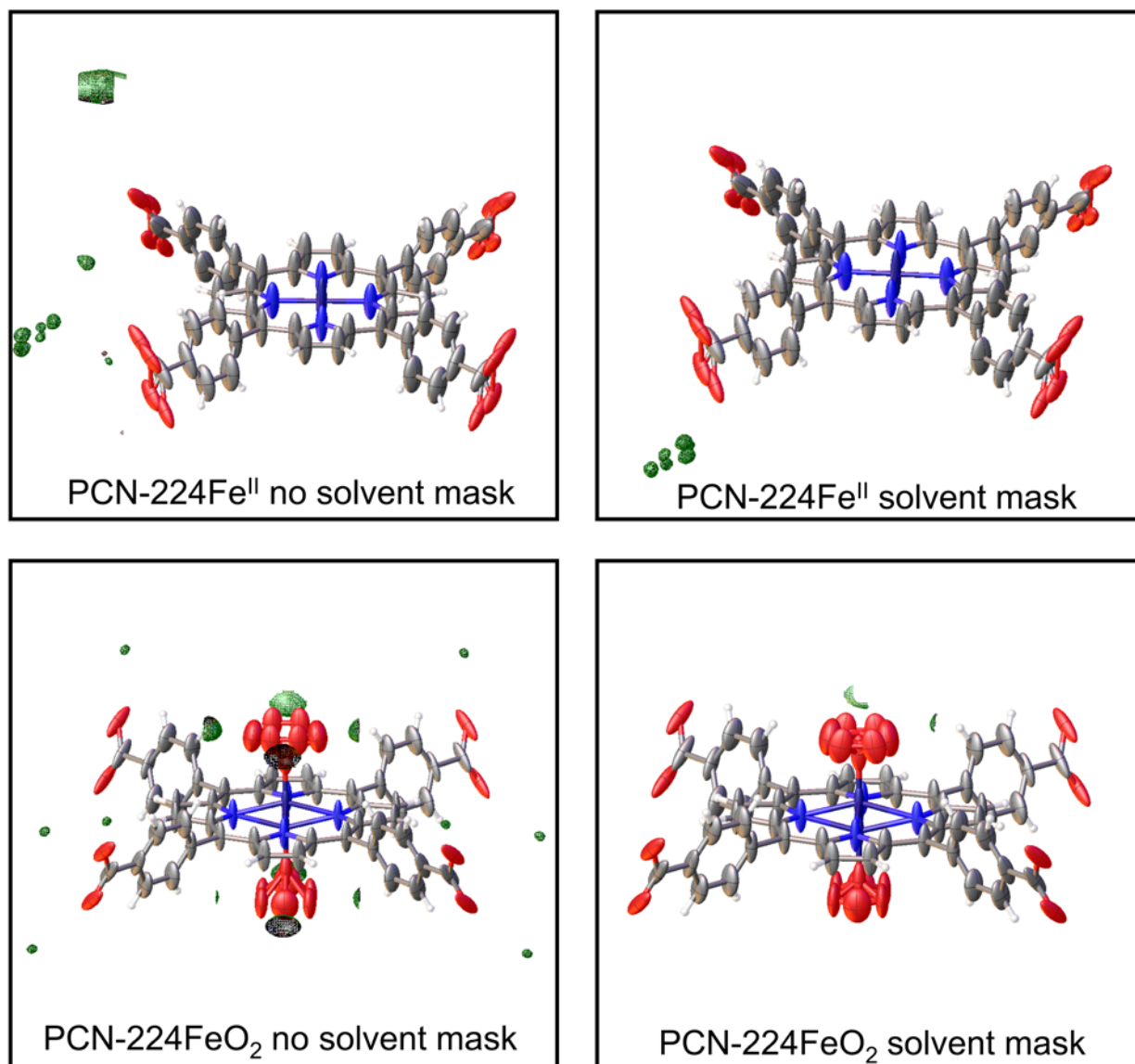


**Figure S2** | Residual electron density plots for **1** and **2** both before and after application of a solvent mask. Grids for plotting were set at 0.1 e<sup>-</sup>/Å and generated with the Olex program package.

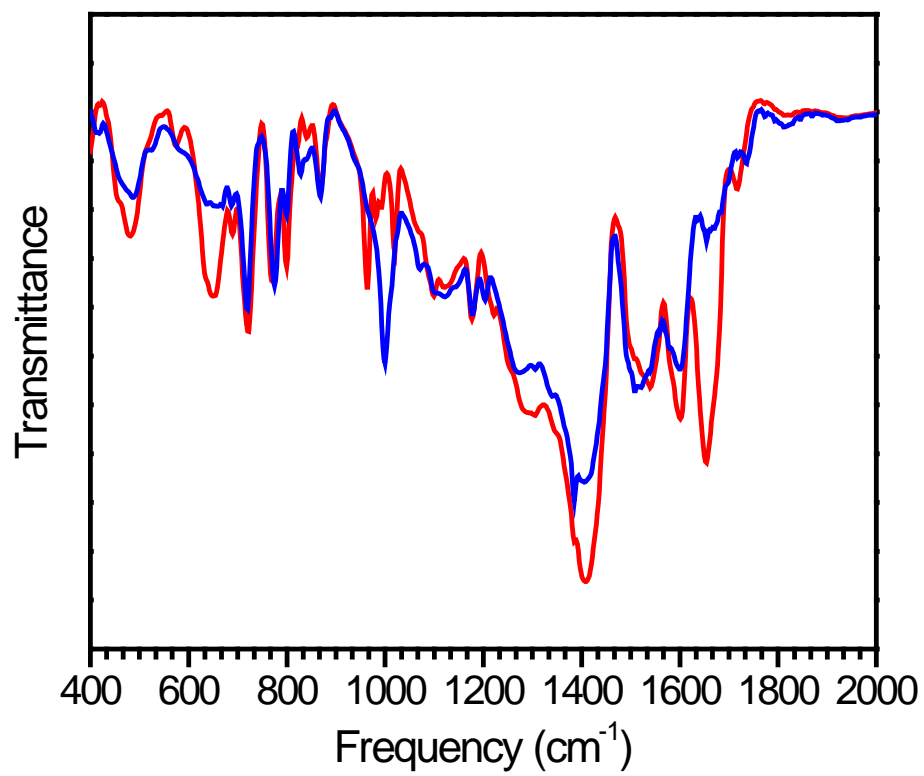


**Figure S3** | IR spectra of KBr pellets of PCN-224 (red) and **1** (blue).

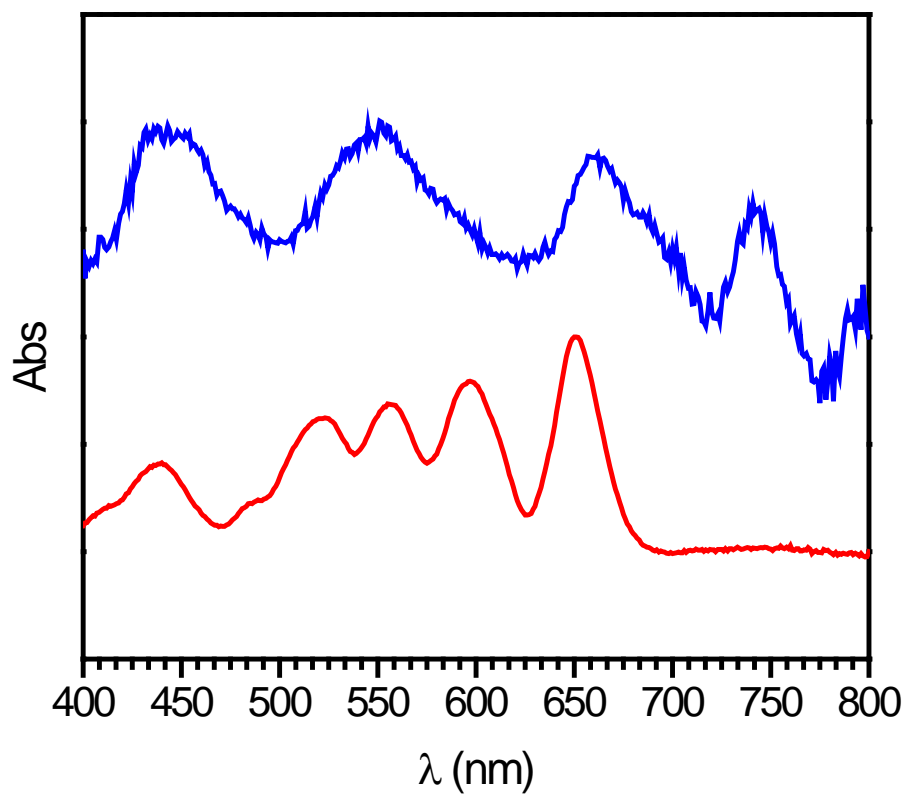


**Figure S4** | Diffuse reflectance UV-Vis spectra of PCN-224 (red) and **1** (blue).



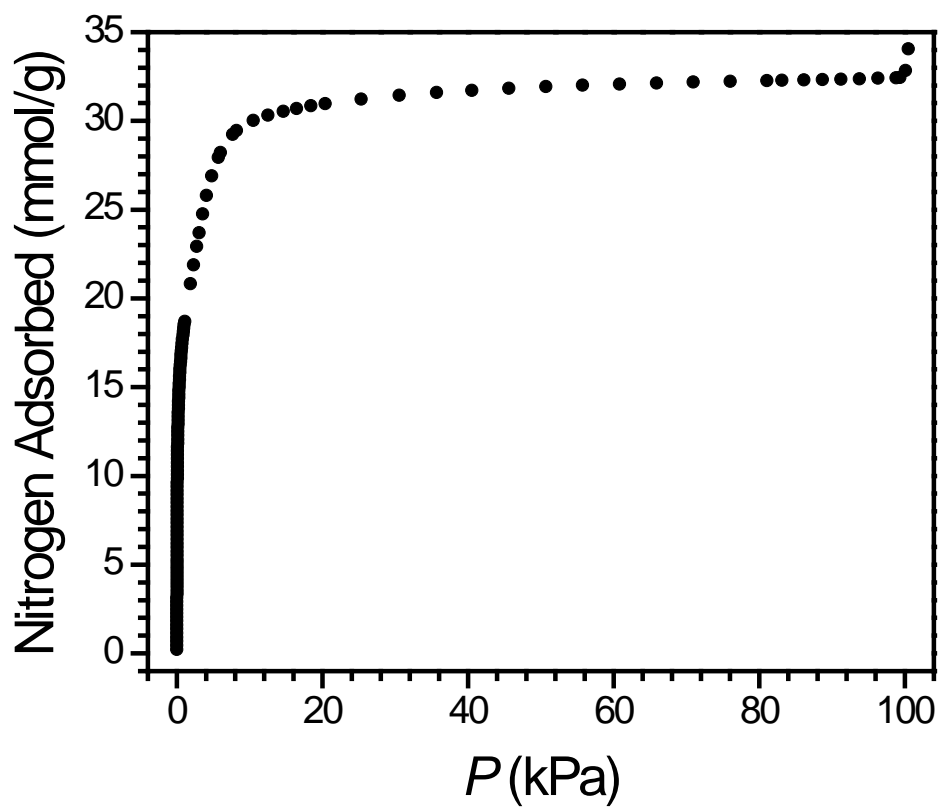


**Figure S5** |  $N_2$  adsorption data for **1** at 77 K.

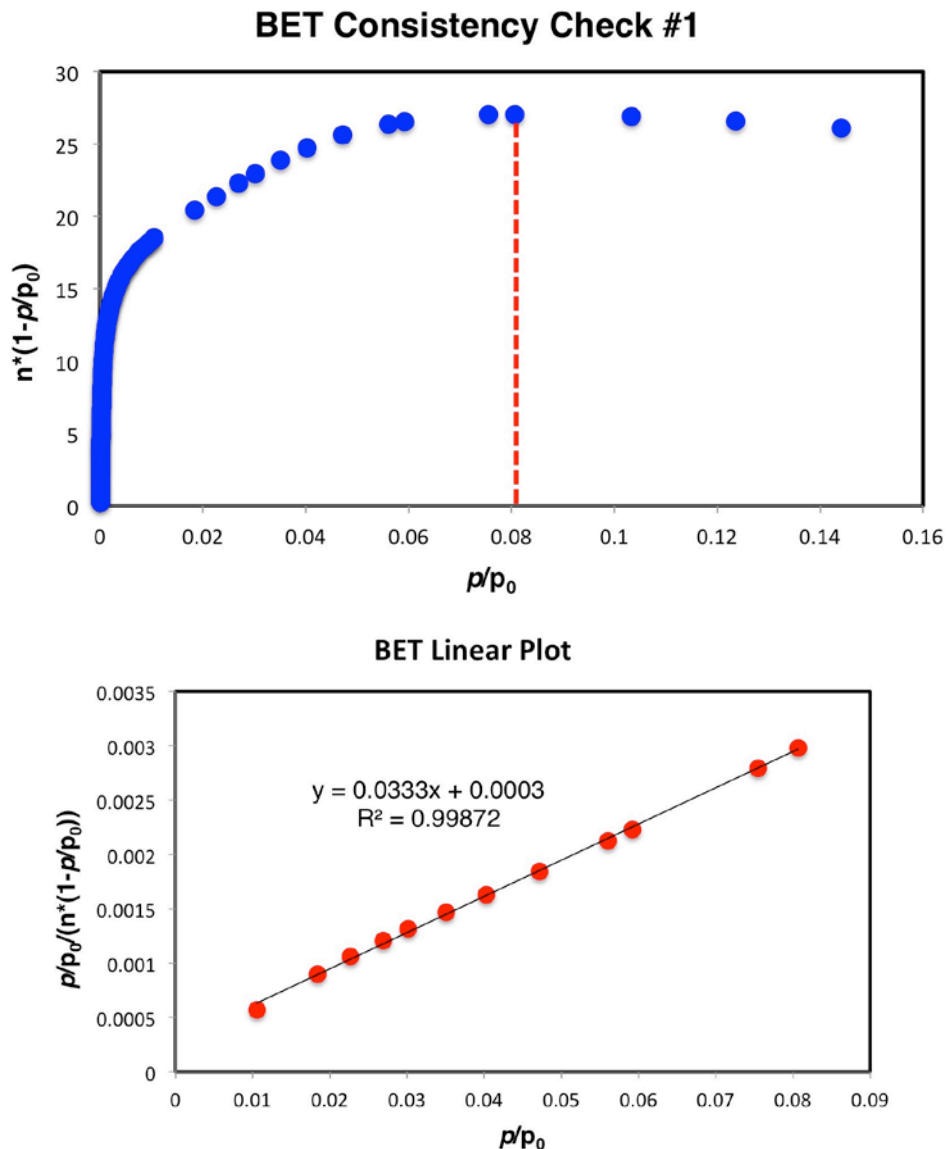


**Figure S6** | Determination of BET surface area for **1**. Top: Plot of  $n \cdot (1 - p/p_0)$  vs.  $p/p_0$  to determine the maximum  $p/p_0$  used in the BET linear fit according to the first BET consistency criterion.<sup>10</sup> Bottom: Plot of  $p/p_0 / (n \cdot (1 - p/p_0))$  vs.  $p/p_0$  to determine the BET surface area.<sup>10</sup> The slope of the best fit line for  $0.01 < p/p_0 < 0.08$  is 0.033, and the y-intercept is  $2.8 \times 10^{-4}$ , which satisfies the second BET consistency criterion. This results in a saturation capacity of 29.7 mmol/g and a BET surface area of 2901(32) m<sup>2</sup>/g.

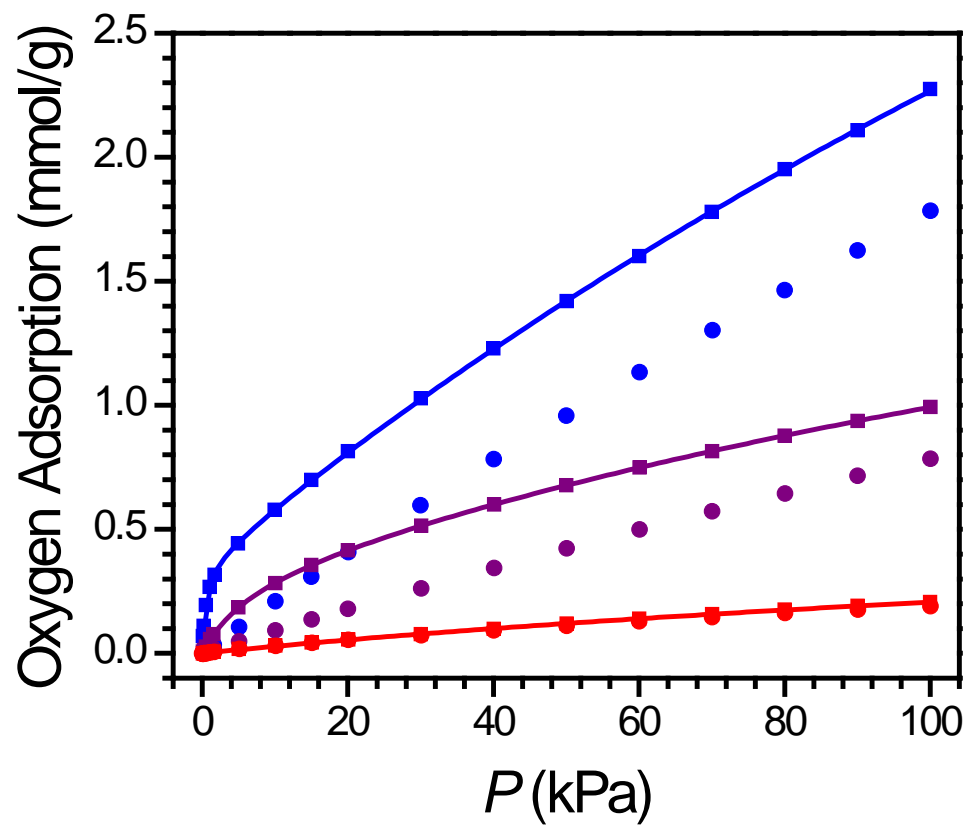


**Figure S7** | Oxygen adsorption data for **1** (squares) and PCN-224 (circles) at 298 K (red), 226 K (purple), 195 K (blue). Solid lines correspond to fits using a dual-site Langmuir model.

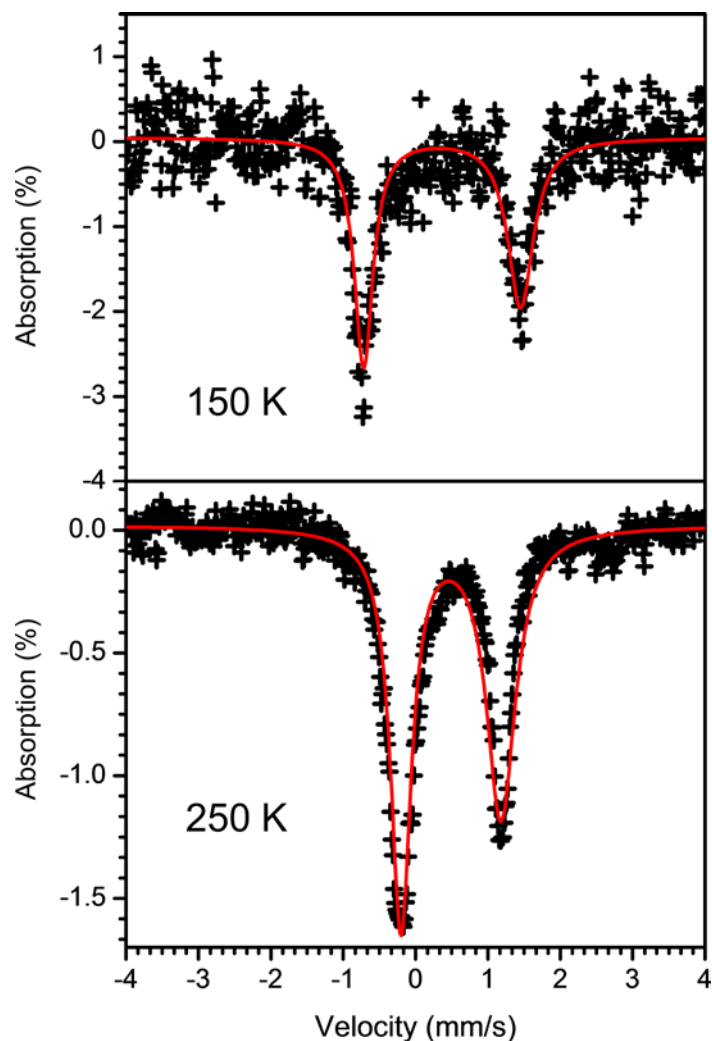


**Figure S8** | Mössbauer spectrum for **2** collected at 150 and 250 K. The primary observed species is **1** at 150 K with fit parameters of  $\delta = 0.37(2)$  mm/s and  $\Delta E_Q = 2.17(4)$  mm/s. Upon warming to 250 K only **1** is observed with fit parameters of  $\delta = 0.489(5)$  mm/s and  $\Delta E_Q = 1.38(1)$  mm/s.

**Table S1** / Crystal data and structure refinement for **1**.

Identification code	PCN-224Fe <sup>II</sup>
Empirical formula	C <sub>144</sub> H <sub>72</sub> Fe <sub>3</sub> N <sub>12</sub> O <sub>64</sub> Zr <sub>12</sub>
Formula weight	4256.32
Temperature/K	100
Crystal system	cubic
Space group	<i>Im-3m</i>
a/Å	38.4265(16)
b/Å	38.4265(16)
c/Å	38.4265(16)
$\alpha/^\circ$	90
$\beta/^\circ$	90
$\gamma/^\circ$	90
Volume/Å <sup>3</sup>	56740(7)
Z	4
$\rho_{\text{calc}}/\text{g}/\text{cm}^3$	0.498
$\mu/\text{mm}^{-1}$	2.553
F(000)	8360.0
Crystal size/mm <sup>3</sup>	0.3 × 0.3 × 0.3
Radiation	CuK $\alpha$ ( $\lambda$ = 1.54178)
2 $\Theta$ range for data collection/ $^\circ$	3.252 to 136.398
Index ranges	-45 ≤ h ≤ 36, -44 ≤ k ≤ 46, -45 ≤ l ≤ 46
Reflections collected	322200
Independent reflections	4847 [ $R_{\text{int}}$ = 0.0537, $R_{\text{sigma}}$ = 0.0196]
Data/restraints/parameters	4847/264/128
Goodness-of-fit on F <sup>2</sup>	1.106
Final R indexes [ $I \geq 2\sigma(I)$ ]	$R_1$ = 0.0704, $wR_2$ = 0.2293
Final R indexes [all data]	$R_1$ = 0.0841, $wR_2$ = 0.2428
Largest diff. peak/hole / e Å <sup>-3</sup>	1.18/-0.43

**Table S2** / Crystal data and structure refinement for **2**.

Identification code	PCN-224FeO <sub>2</sub>
Empirical formula	C <sub>18</sub> H <sub>9</sub> N <sub>1.5</sub> O <sub>8.75</sub> Fe <sub>0.38</sub> Zr <sub>1.5</sub>
Formula weight	544.04
Temperature/K	100
Crystal system	cubic
Space group	<i>Im-3m</i>
a/Å	38.6484(19)
b/Å	38.6484(19)
c/Å	38.6484(19)
$\alpha/^\circ$	90
$\beta/^\circ$	90
$\gamma/^\circ$	90
Volume/Å <sup>3</sup>	57729(9)
Z	32
$\rho_{\text{calc}}/\text{g}/\text{cm}^3$	0.501
$\mu/\text{mm}^{-1}$	2.522
F(000)	8552.0
Crystal size/mm <sup>3</sup>	0.3 × 0.3 × 0.3
Radiation	CuK $\alpha$ ( $\lambda$ = 1.54178)
2 $\Theta$ range for data collection/ $^\circ$	3.232 to 130.086
Index ranges	-45 ≤ h ≤ 44, -44 ≤ k ≤ 45, -41 ≤ l ≤ 45
Reflections collected	184326
Independent reflections	4616 [ $R_{\text{int}}$ = 0.0410, $R_{\text{sigma}}$ = 0.0112]
Data/restraints/parameters	4616/274/140
Goodness-of-fit on F <sup>2</sup>	1.091
Final R indexes [ $I \geq 2\sigma(I)$ ]	$R_1$ = 0.0444, $wR_2$ = 0.1389
Final R indexes [all data]	$R_1$ = 0.0498, $wR_2$ = 0.1422
Largest diff. peak/hole / e Å <sup>-3</sup>	0.81/-0.33

**Table S3** / Parameters for dual-site Langmuir fits for O<sub>2</sub> uptake by **1** at selected temperatures.

T (K)	q <sub>sat1</sub> (mmol/g)	B <sub>01</sub> (kPa <sup>-1</sup> )	E <sub>1</sub> (J)	q <sub>sat2</sub> (mmol/g)	B <sub>02</sub> (kPa <sup>-1</sup> )	E <sub>2</sub> (J)
141	666	2.4E-8	10250	0.519	2.7E-9	32270
156	664	2.4E-8	10000	0.55	8.2E-8	28320
195	677	4.3E-8	10420	0.5	4E-8	27390
226	670	3.6E-8	10170	0.5	1.6E-8	29070
273	676	4.5E-8	10380	0.54	1.6E-8	29750
298	672	3.9E-8	10250	0.5	1.6E-8	29860

## References

- (1) Feng, D.; Chung, W.-C.; Wei, Z.; Gu, Z.-Y.; Jiang, H.-L.; Chen, Y.-P.; Darensbourg, D. J.; Zhou, H.-C. *J. Am. Chem. Soc.* **2013**, *135*, 17105.
- (2) Sheldrick, G. M. SADABS, version 2.03, Bruker Analytical X-Ray Systems, Madison, WI, 2000.
- (3) Sheldrick, G. M., SHELXTL, Version 6.12; Bruker Analytical X-ray Systems, Inc.: Madison, WI, 2000.
- (4) Dolomanov, O. V.; Bourhis, L. J.; Gildea, R. J.; Howard, J. A. K.; Puschmann, H. *J. Appl. Crystallogr.* **2009**, *42*, 339.
- (5) Muller, P.; Herbst-Irmer, R.; Spek, A.; Schneider, T.; Sawaya, M. *Crystal Structure Refinement: A Crystallographer's Guide to SHELXL*; OUP Oxford, 2006.
- (6) Morris, W.; Voloskiy, B.; Demir, S.; Gándara, F.; McGrier, P. L.; Furukawa, H.; Cascio, D.; Stoddart, J. F.; Yaghi, O. M. *Inorg. Chem.* **2012**, *51*, 6443.
- (7) Düren, T.; Millange, F.; Férey, G.; Walton, K. S.; Snurr, R. Q. *J. Phys. Chem. C* **2007**, *111*, 15356.
- (7) Nasset, M. J. M.; Shokhirev, N. V.; Enemark, P. D.; Jacobson, S. E.; Walker, F. A. *Inorg. Chem.* **1996**, *35*, 5188.
- (9) Wu, Y.; Komatsu, T.; Tsuchida, E. *Inorg. Chim. Acta* **2001**, *322*, 120.
- (10) Walton, K. S.; Snurr, R. Q. *J. Am. Chem. Soc.* **2007**, *129*, 8552.